

2012



RECENT DEVELOPMENTS IN METALLURGY, MATERIALS AND ENVIRONMENT

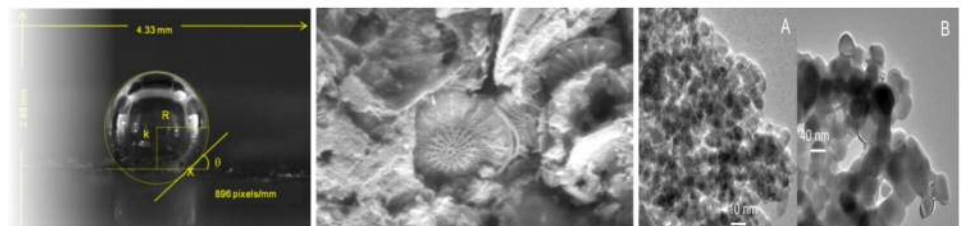
CHAPTER 10

Mathematical Modeling of Temperature for the Deposition of Particles of Fe-Cr-Mo on Tool Steel D2 by HVOF

*C. A. Guevara Chávez¹, J. L. Acevedo Dávila¹,
P. Hernandez Gutierrez¹, F. Cepeda Rodriguez¹.*

¹CORPORACIÓN MEXICANA DE INVESTIGACIÓN EN MATERIALES S.A. DE C.V.

ISBN 978-607-9023-18-8



Materials

CHAPTER 10

Mathematical Modeling of Temperature for the Deposition of Particles of Fe-Cr-Mo on Tool Steel D2 by HVOF

C. A. Guevara Chávez¹, J. L. Acevedo Dávila¹, P. Hernandez Gutierrez¹, F. Cepeda Rodriguez¹.

¹Corporación Mexicana de Investigación en Materiales S.A. de C.V. Investigación y Desarrollo Tecnológico, Ciencia y Tecnología # 790, Fracc. Saltillo 400. Saltillo, Coahuila, México Código postal 25290.

Abstract

This research examined the influence of process parameters influencing the deposit of a coating structure Diamalloy 1008 (Fe-Cr-Mo alloy mixture) applied by oxy-fuel high-speed (HVOF) on steel samples grade D2 tool. This type of coating is commonly used as protection against wear and corrosion. But it has the ability to rebuild areas damaged by weathering and erosion. The formulation of the mathematical model of the temperature with respect to the deposition of repair material on the substrate prior to impact, to assess the behavior of the particle trajectory, in order to predict the behavior under the conditions of liquid, slurry and solid.

Keywords: Mathematical model, HVOF, Coating.

1. Introduction

The alloys Fe-Cr-Mo are used in coatings for the protection of components subject to wear and corrosion [1]. Thermal spray coatings at high speed (HVOF, for its acronym in English) in alloys Fe-Cr-Mo have been reported with good results in the field of projections for grade steels for cold work tool [2]. The HVOF is an attractive method for applying solder coating and retrieve diameters. New surfaces can be provided free of weld distortion [3]. For those materials that are susceptible to cracking and changes in the composition due to the formation of very hard phases and the high carbon content, due in turn to the process conditions, which combine a relatively low temperature flame with a short time exposure [4]. This method uses high pressure fuel (propylene, acetylene, propane or hydrogen) to produce temperatures above 3029 K and to generate a supersonic flow of gas, about 2000 m / s [5]. The microstructure and physical properties of the coatings are determined by physical and chemical properties of the particles impregnated in the substrate, which in turn is dependent on a large number of parameters as the design of the gun, the fuel / oxygen the relative

position of the substrate with respect to the gun, the injection method, the size and shape of particle among others [6]. The particle trajectory, velocity and impact the state in which the substrate is critical because the conditions of adhesion of the same and its effect on the application of the coating [7, 8]. The temperature of the particles and the speed of these control the microstructure, porosity, hardness and adhesion of the coating [9, 10]. Some studies have estimated mathematical models for the dynamics of particles and gas during the HVOF process [10-13], but except for the numerical work of Oberkampf and Talpallikar [11] are made stationary character approaches [10, 13] for temperature, without considering the time of the resulting functions. In this paper, mathematical modeling by considering the Fourier equation in one dimension to analyze the temperature in the direction of application.

2. Experimental procedures

2.1 Materials and equipment

The selection of a coated material and supply of welding involves more than adequate choice of the desired properties of the deposit. Consideration of this should be given to the conditions, and the role and service of the environment, in addition to the physical and chemical properties of the coating and substrate supply. The use of substrates such as tool steel for cold working, were repaired using also a "tool steel corresponding" powder (Fe-Cr-Mo) to repair materials for the case of HVOF. All samples have the same overall dimensions are rectangular blocks of 1 "(25.4 mm) long by ¼" (6.35 mm) in height.

The samples were machined, degreased and shot blasted with sand of aluminum oxide immediately before spray coating. Samples were preheated at a temperature range of 250 to 350 ° C using flame HVOF gun and a gas torch, this to reduce the difference in thermal expansion between the solder and the substrate. They were then covered with the repair material and welding the entire upper surface of the sample to thicknesses in the range 0.5 to 1.5 mm. The HVOF process was carried out according to the parameters spray listed in the Table 1.

Variable	Low level	Medium level	High level
Relationship fuel / oxygen	0,30	0,40	0,50
Distance (mm)	200	225	250

Table 1. Experimental conditions for the HVOF process.

The gas atomized powder commercial Fe-Cr-Mo was provided by Sulzer Metco Inc. The chemical composition and particle size are shown in Table 2. The team Sulzer Metco Diamond Jet DJ 2700 Gun was used for powder application, injecting gas propylene. The powder was fed through the injection of nitrogen at a flow rate of 47 g / min.

Powder	Composition (weight %)							Nominal particle size (µm)
	Cu	Cr	Mo	Mn	Si	B	Fe	
Fe-Cr-Mo	3	17	11	0.1	3	3	Bal.	-45 +/-5.5 µm

Table 2. Specification of the powder used in the application by the HVOF technique on samples of D2 tool steel.

An experimental design was Taguchi type used in the study to evaluate the effect of the two parameters (relative flow of the fuel / oxygen, and working distance) on the trajectory of the particles in terms of speed and temperature of the same as shown in Table 3.

Parameter Test	Fuel Flow (SLPM*)	Oxygen Flow (SLPM*)	Distance (mm)	Relationship fuel / oxygen
1	85	240	200	0,30
2	85	240	225	0,30
3	85	240	250	0,30
4	85	210	200	0,40
5	85	210	225	0,40
6	85	210	250	0,40
7	85	170	200	0,50
8	85	170	225	0,50
9	85	170	250	0,50

*Standard liters per minute

Table 3. Design of experiments type Taguchi.

Once coated and welded samples were prepared metallographically to ASTM E-3. Samples polished to a mirror finish were etched under the ASTM E-407. In order to disclose the use Picral microstructure and 4% HCl, then hardness test performed on the coating, base material and the welding under the ASTM E-384, with a diamond indenter with an angle of 136 ° in Hv500 scale with a load of 500 grf. With equivalence HRC Finally, analysis was performed deposit on the substrate using a scanning electron microscope Jeol mark in order to evaluate the quality of the joint.

2.2 Formulation of the mathematical model

To formulate the mathematical model of the system shown in Figure 1, the substrate must be fixed on the table, which has three degrees of freedom and allows the movement of the given substrate at a uniform speed, and material flow coating is constant, to ensure a uniform thickness throughout its length. For this mathematical model are taking the following conditions given by the experimental design and the nature of the process.

- It is assumed that the coated particle travels along the centerline of the gas flow.
- As the working distance is 200 mm and the gas flow is supersonic, it is assumed that its speed is constant, its density and temperature.
- The particle is spherical.
- The transfer of momentum between particles is negligible.
- The melting and solidification of the coating on the substrate depend on the power of the gun.
- Relative motion between the coating material is fed and the substrate.

The molten coating material is atomized and deposited on the substrate surface as a puddle. The coating is deposited on the substrate is approximately semicylindrical and is represented in Figure 2. The coating applied on the substrate is divided into three zones (liquid coating, coating and coating solidifies solid). The heat transfer equations are used to predict behavior in these three areas, subject to the following considerations and boundary conditions:

- 1 - The conductivity and thermal diffusivity of the coating material are averages of the components.
- 2 - The mass diffusivity of each element in the liquid phase is the average value of the self-diffusion under the local temperature and initial temperature.
- 3 - The coating and substrate are in perfect thermal contact.
- 4 - No mass self-diffusion in the solid phase.
- 5 - No convection in the liquid phase.
- 6- The molten coating is a uniform solution of composition equal to the initial mixing, solidification begins immediately.

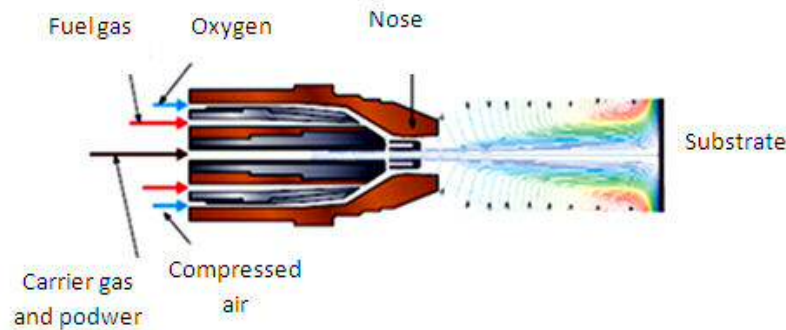


Figure 1. Schematic HVOF

With the above considerations, the equations of heat transfer in the substrate, the solidification zone and the zone of the coating liquid and the mass transfer equation is used to determine the distribution of solute atoms in the solid phase , The model for the three areas and other auxiliary conditions are formulated as follows:

a) Equations based on heat transfer

$$\frac{\partial^2 T}{\partial x^2} = \frac{1}{\alpha} \frac{\partial T}{\partial t} \quad (1)$$

- Solid coating zone

$$t \geq 0 \quad 0 \leq x \leq a$$

$$\frac{\partial^2 T_1}{\partial x^2} = \frac{1}{\alpha} \frac{\partial T_1}{\partial t} \quad (2)$$

- Area of solidification of the coating

$$t \geq 0 \quad 0 \leq x \leq s(t)$$

$$\frac{\partial^2 T_2}{\partial x^2} = \frac{1}{\alpha_2} \frac{\partial T_2}{\partial t} \quad (3)$$

- Coating liquid Area
 $t \geq 0 \quad s(t) \leq x \leq b$

$$\frac{\partial^2 T_3}{\partial x^2} = \frac{1}{\alpha_3} \frac{\partial T_3}{\partial t} \quad (4)$$

b) auxiliary conditions

$$K_1 \frac{\partial T_1}{\partial x} = h_1(T_1 - T_0) \quad (5)$$

$x = 0 \quad y \geq 0,$

$$T_1(a, t) = T_2(a, t) \quad (6)$$

$$K_1 \frac{\partial T_1}{\partial x} = K_2 \frac{\partial T_2}{\partial x} \quad (7)$$

$x = a \quad y \geq 0$

$$T_2[s(t), t] = T_3[s(t), t] = T_1[c_t, s(t)] \quad (8)$$

$x = b \quad y \geq 0$

$$K_3 \frac{\partial T_3}{\partial x} = h_3(T_3 - T_1) \quad (9)$$

$x = b \quad y \geq 0$

$$K_2 \frac{\partial T_2}{\partial x} = K_3 \frac{\partial T_3}{\partial x} = \rho c_t \frac{ds}{dt} \quad (10)$$

$x = s(t) \quad y \geq 0 \quad s(0) = a$

The conditions given by equations (1) to (3) and the auxiliary conditions (4) to (10) are made on the basis of the following considerations: The initial temperature T_3 is given by $T_3 = T_p + 150 \text{ }^\circ\text{C}$, where T_p is the melting temperature of the coating material, which adds 100 to 150 $^\circ\text{C}$ more to keep the liquid phase completely. Figure 2 shows the one-dimensional graphical representation of the problem.

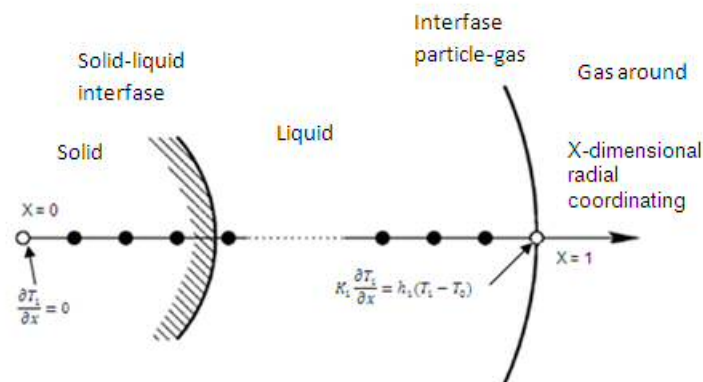


Figure 2. Dimensional graphical representation of the problem

3. Results and discussion

Once applied the weld by conventional HVOF process not using the parameters listed in Table 1, proceeded to characterize the samples (optical microscopy, hardness, chemical) found as follows; Metallographic analysis according to ASTM E-3, E-407 revealed a matrix microstructure consisting of a tempered martensite with carbides of chromium and molybdenum and $M_{23}C_7$ M_7C_6 dispersed in the matrix base material, with grain growth in the direction $\langle 100 \rangle$ in the heat affected zone and an array of columnar grains of solidification, and interdendritic precipitation of primary carbides in the weld zone. See Figure 3.



Figure 3. Tempered martensite with carbides $M_{23}C_7$ and Chromium and Molybdenum matrix dispersed M_7C_6 .

We proceeded to determine the properties of the base material to select the powdered material to coat by the HVOF technique, the results of hardness and chemical analysis. Hardness test according to ASTM E-384, see table 4. The chemical analysis according to ASTM E-1019, E-1085 was performed using the technique of X-ray spectrometry and determination of C and S for the combustion technique and infrared detection. See Table 5.

Sample	Hv ₅₀₀						Average (H v ₅₀₀)	Equivalence (HRC)
	696	686	684	694	688	670		
base Metal	696	686	684	694	688	670	686	59
AISI D2	58-64 HRC							

Table 4. Hardness of the base metal and its equivalence according to the specification for a tool steel for cold working.

Identification	% Element					
	C	S	Mo	P	V	Cr
base Metal	1,56	0,017	0,96	0,011	0,84	11,53

Table 5. Chemical composition of the base material.

After adjusting the conditions of application of HVOF, at this stage tests were conducted 9 by varying the different parameters of projection welding as shown in Table 3. In the present study evaluated the effect of distance with respect to joining the deposit on the substrate and the adhesion thereof, and the amount of oxide present at the interface of the coating and substrate. In Figure 4 shows the adhesion of deposit to a distance of 200 mm with a ratio of fuel / oxygen of 0.30 found a good deposition of the repair material into the substrate of tool steel for cold working. See Table 6. Finding a hardness Hv tank 579 as shown in Table 7. In Figure 5. It is observed that there is a small amount of porosity in the cross section of the tank which is consistent with the parameters used so that the adhesion of the repair material to the substrate can be considered good because there is a considerable amount of oxides that can act as stress concentrators and weaken the union. In Figure 6. Shows the adhesion of deposit to a distance of 250 mm with a ratio of fuel / oxygen of 0.50 found

a coating density greater than in previous case which generates a repair material deposition. See Table 7. Finding a hardness Hv tank 661 as shown in Figure 8. In Figure 9. It is observed that there is a large amount of porosity in the cross section of the tank which is consistent with the parameters used so that the adhesion of the repair material to the substrate is poor due to the formation of an oxide layer at the interface of the base material and repair material, which generates a detachment zone materials susceptible to damage by corrosion.

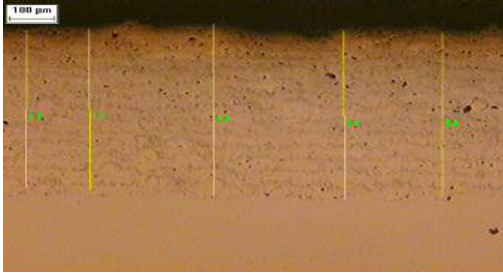


Figure 4. Surface appearance of the coating. 50X

Test (µm)					Average (µm)
506	517	554	543	528	529,6

Table 6. Thickness of the deposit in the substrate.

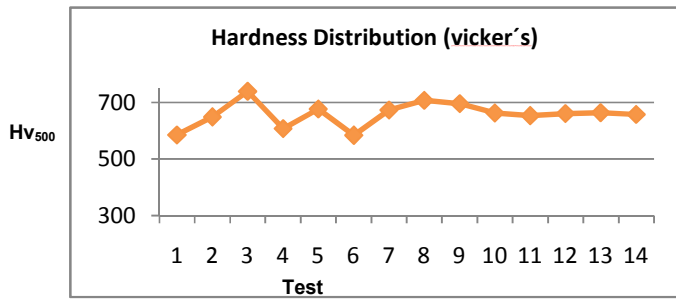


Figure 5. Hardness Hv500 distribution in the substrate coating tool steel for Cold work.

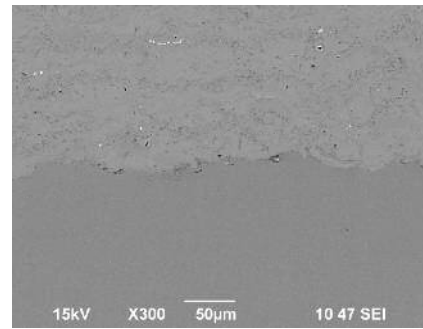


Figure 6. Scanning electron microscopy (SEM), porosity of the deposit.

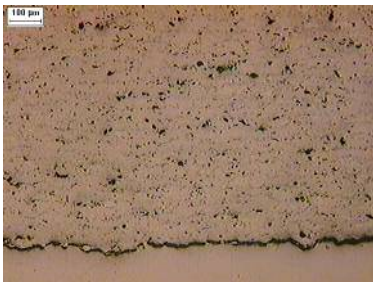


Figure 7. Surface appearance of the coating. 50X

Test (µm)					Average (µm)
669	653	661	664	658	661

Table 7. Thickness of the deposit in the substrate.

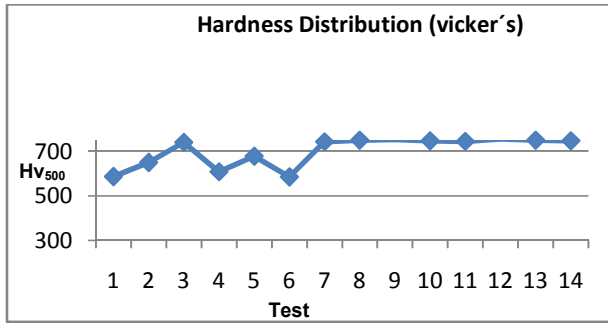


Figure 8. Hardness Hv500 distribution in the substrate coating tool steel for Cold work.

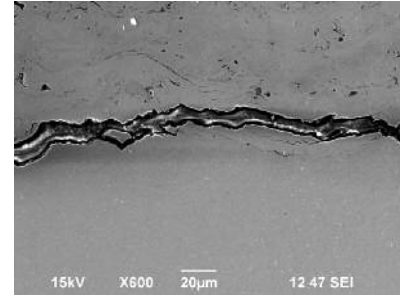


Figure 9. Scanning electron microscopy (SEM), porosity of the deposit.

Once obtained satisfactory results as to the binding is concerned, it is appropriate to obtain the equation simplifies the effect of temperature and speed in the trajectory of the particle prior to impact, i.e. to obtain a coating density where there is no oxidation at the interface of the materials. For the area of solid coating gives the following expression for the temperature:

$$T_1(x, t) = 3029 e^{-\frac{7.2 \cdot 10^3 \alpha t}{a^2}} \cos\left(\frac{84.8x}{a}\right) \text{ para } 0 \leq x < a$$

For the solidification zone of the coating is:

$$T_2(x, t) = e^{-\frac{7.2 \cdot 10^3 \alpha t}{a^2}} \left\{ \left[\frac{257 \cdot 10^3 K_1}{\gamma K_2} \text{sen}(\gamma) - 274.5 \cos(\gamma) \right] \cos\left(\frac{\gamma}{a}x\right) + \left[274.5 \text{sen}(\gamma) - \frac{257 \cdot 10^3 K_1}{\gamma K_2} \cos(\gamma) \right] \text{sen}\left(\frac{\gamma}{a}x\right) \right\} \text{ para } a \leq x < s(t)$$

Where:

$$\gamma = 84.8 \sqrt{\frac{\alpha_1}{\alpha_2}}$$

For the liquid zone of the coating is:

$$T_3(x, t) = e^{-\frac{7.2 \cdot 10^3 \alpha t}{a^2}} \left\{ G \cos\left(\frac{\gamma_2}{a}x\right) + H \text{sen}\left(\frac{\gamma_2}{a}x\right) \right\} \text{ para } s(t) \leq x < b$$

Where:

$$G = -\frac{\varepsilon}{\gamma_2 K_3} \text{sen}(\gamma_2) - 137.3 [\cos(2\gamma_1 + \gamma_2) + \cos(2\gamma_1 - \gamma_2)]$$

$$H = \frac{\varepsilon}{\gamma_2 K_3} \cos(\gamma_2) - 137.3 [\text{sen}(2\gamma_1 + \gamma_2) + \cos(\gamma_2 - 2\gamma_1)]$$

$$\varepsilon = 274.5 \gamma_1 K_2 \text{sen}(2\gamma_1) - 257 \cdot 10^3 K_1$$

$$\gamma_1 = 84.8 \sqrt{\frac{\alpha_1}{\alpha_2}}$$

$$\gamma_2 = 84.8 \sqrt{\frac{\alpha_1}{\alpha_3}}$$

4. Conclusions

The mathematical model establishes the temperature and velocity conditions affecting repair material deposition on the substrate and its influence in the path state under the conditions of liquid and solid slurry, thus validating the speed of the substrate, power of the gun, specific heats, heats of fusion, thermal conductivity and density of the components of the coating.

Taguchi design of experiments to identify the flow of fuel, distance, and the oxygen flow as HVOF process parameters affecting major particle deposition is "on path", i.e. before impact.

The analysis by the technique of Scanning Electron Microscopy (SEM) showed that the repair material deposited on the substrate contains a low amount of rust due to the ratio of fuel / oxygen used was the lowest (0.30). Therefore, within the range explored, the porosity is more closely related to the fuel-oxygen ratio of impacting the density of the coating deposited.

Oxide content increase as fuel ratio was higher in its oxygen content, said oxidation affects the adhesion of the repair material into the substrate, causing stress concentrators sites which would foster a detachment of the tank when this is subjected to tension.

This type of coating has been successfully adhered to the material obtaining a stool within the ranges of 500 to 700 microns. The hardness test showed that the powder coating selected for this application complies with the original properties of the tooling may well return to service tooling.

References

1. Ebner R., Leitner H., Jeglitsch F., Caliskanoglu D., *5th International Conference on Tooling*, **1999**, 56-59.
2. Cary Howard B., *Modern Welding Technologies*, Regents Prentice Hall, New Jersey, **2004**, 176-181.
3. Doyen P.S., Skrabec Q. R., (1997), A new technique for welding tool steel, *The Welding Journal*, **60**(9), 25 – 28.
4. Losano G., Morgenfeld J., (2001), Criterios para evaluar el riesgo de fisuración en caliente, *Revista Soldadura*, **4**(11), 326-327.
5. Beardsley M.B.,(1997), Think thermal barrier, *Coatings for diesel engines*, **6**(2), 181-186.
6. Saaedi J., Coyle T. W., Mostaghimi J., (2009), Effects of HVOF Process Parameters on the properties of Ni-Cr coatings, Centre for Advanced Coating Technologies, *Department of Materials Science and Engineering University of Toronto, Toronto, Canada*, 196-199.
7. Gutierrez-Miravete Llavernia, Trapaga G.M., Szekely J., Grant N.J., (2006), A Mathematical Model of the Spray Deposition Process.
8. Tan J.C, Looney L., (1991), Component repair using HVOF thermal spraying, *Materials processing research centre*, **93**(93), 203-208.

9. Tawfik H.H., Zimmerman F., (1997), Mathematical modeling of the gas and powder flow in HVOF systems, *Journal of thermal spray technology*, **6**(3), 345-352.
10. Katanoda H., Kiriaki T., Tachibanaki T., Kawakita J., Kuroda S., Fukuhara M., (2009), Mathematical modeling and experimental validation of the warm spray (two-stage HVOF), *Journal of thermal spray technology*, **18**(3), 401-410.
11. Oberkampf W. L., Talpallikar M., (1996), Analysis of a High-Velocity Oxygen-Fuel (HVOF) Thermal Torch Part 1: Numerical Formulation, *Journal of thermal spray technology*, **5**(1), 53-61.
12. Ivošević M., Gupta V., Baldoni J.A., Cairncross R.A., Twardowski T.E., Knight R., Effect of Substrate Roughness on Splating Behavior of HVOF Sprayed Polymer Particles: Modeling and Experiments, (2006), *Journal of thermal spray technology*, **15**(4), 725-730.
13. Tawfik H.H., Zimmerman F., Mathematical Modeling of the Gas and Powder Flow in HVOF Systems, (1997), *Journal of thermal spray technology*, **6**(3), 345-352.